Received: 5 April 2023 | Revised: 5 May 2023 | Accepted: 8 May 2023

DOI: 10.1111/jfd.13799

Journal of Fish Diseases WILEY

RESEARCH ARTICLE

Alteration of synergistic immune response in gut–liver axis of white crucian carp (*Carassius cuvieri*) after gut infection with *Aeromonas hydrophila*

Fei Wang[1] | **Zi-Le Qin**[1] | **Wei-Sheng Luo**[1] | **Ning-Xia Xiong**[1] | **Ming-Zhu Huang**[2] | **Jie Ou**[1] | **Sheng-Wei Luo**[1] | **Shao-Jun Liu**[1]

[1]State Key Laboratory of Developmental Biology of Freshwater Fish, College of Life Science, Hunan Normal University, Changsha, China

[2]National R&D Center for Freshwater Fish Processing, Jiangxi Normal University, Nanchang, China

Correspondence
Sheng-Wei Luo, College of Life Science, Hunan Normal University, Changsha 410081, China.
Email: swluo1@163.com; swluo@hunnu.edu.cn

Funding information
National Natural Science Foundation of China, China, Grant/Award Number: 31902363; Hunan Provincial Natural Science Foundation of China, China, Grant/Award Number: 2021JJ40340

Abstract

Aeromonas hydrophila can pose a great threat to the survival of farmed fish. In current study, we investigated the pathological characteristics and immune response in gut–liver axis of white crucian carp (WCC) upon gut infection. WCC anally intubated with *A. hydrophila* exerted a tissue deformation in damaged midgut with elevated levels of goblet cells along with a significant decrease in tight junction proteins and villi length-to-width ratios. In addition, immune-related gene expressions and antioxidant properties increased dramatically in gut–liver axis of WCC following gut infection with *A. hydrophila*. These results highlighted the immune modulation and redox alteration in gut–liver axis of WCC in response to gut infection.

KEYWORDS
antioxidant status, crucian carp, gene expressions, gut infection

1 | INTRODUCTION

Exposure to environmental pollutants enhance incidence of infectious diseases in mammals (Wen et al., 2022). Similarly, ambient stressors can promote physiological disorder, antioxidant insult and immune suppression in teleost fish, which can enable invasive pathogens to survive and reproduce within the host (Ellis, 1999). Although immunoprophylaxis exerts a great effort in spread restriction of pathogenic diseases, emerging population of resistant bacteria challenged by antibiotics and heavy metal bioaccumulation may elevate the risk for infectious diseases in aquaculture (Dong et al., 2020). Among documented pathogens, *A. hydrophila* is a widespread representative of *Aeromonadaceae* found in aqueous environments and aquatic organisms, which are able to generate a large quantity of virulence factors and bacterial toxins (Awan et al., 2018).

Crucian carp (*Carassius auratus*) is one of popular farmed fish species in China, because of its delicious taste and high-stress resistance (Li, Wang, et al., 2018). However, global climate change may accelerate environmental deterioration and then exacerbate risk factors for emerging diseases in aquaculture (Warner et al., 2010). Thus, farming process of crucian carp is ravaged by microbial infection, which may exhibit an adverse economic impact in aquaculture (Nielsen et al., 2001; Rodger, 2016). Although teleost fish commonly possess a large quantity of pathogen-recognizing receptors (PRRs) and complement components to cope with invasive pathogens (Uribe et al., 2011), pathogens can effectively skirt the elimination of innate immunity and beach mucosal barrier to orchestrate pathogen-induced inflammation for deeper infection (Secombes et al., 2001). Currently, collaborative modulation of gut–liver axis have gradually acquired more attention in fish. Gut–liver axis may refer to reciprocal communication of gut tract, gut microbiota and liver, playing a crucial role in maintaining immune homeostasis (Li, Selmi, et al., 2018). Gut flora is composed of a dynamic community of bacteria, fungi, archaea and protozoans in gut mucosal barrier, which can promote the synthesis of secretory immunoglobulins, recruit activating lymphocytes as well as attenuate pathogenic colonization (Kelly et al., 2005). When gut mucosal barrier function is disrupted, liver can receive endogenous metabolites from gut tract to support

gut–liver connection and detoxify bacterial products under bacteria-induced inflammatory response (Seo & Shah, 2012). However, the synchronous regulation of the gut–liver axis in fish remains unclear.

In this study, the aims were to evaluate gut mucosal barrier function, physiological response and critical gene expressions in midgut and liver of white crucian carp (WCC, *Carassius cuvieri*) after gut infection with *A. hydrophila*, which may give a novel insight into the synchronization of immune regulation in gut–liver axis of *A. hydrophila*-infected fish.

2 | MATERIALS AND METHODS

2.1 | Animal preparation

Healthy WCCs (about 18.24 ± 0.53 g) were daily fed with commercial diets for animal acclimation in clean freshwater until 24 h prior to gut infection with *A. hydrophila* experiment. Fish feed and faeces were removed daily for maintaining water quality during acclimation and infection periods.

2.2 | Bacterial perfusion assay

Aeromonas hydrophila strain L3-3 (NCBI accession number: OM184261) was cultured in Luria-Bertani (LB) medium overnight and then resuspended in 1× PBS (pH 7.3) (Xiong et al., 2022). Then, the previously published gut perfusion method was performed with a slight modification (Song et al., 2014). Briefly, WCCs were anally intubated with *A. hydrophila* (1×10^8 CFU mL^{-1}) in PBS suspension by using a gavage needle inserted into a depth of approximately 3 cm, while equivalent volume of sterile PBS perfusion was used as control group. Tissues (liver, kidney, spleen and midgut) were isolated at 0, 24, 48 and 72 h post-infection, immediately frozen in liquid nitrogen and preserved in −80°C. Each group contained three biological replicates.

2.3 | Histological assay

Midgut samples were fixed in Bouin solution, paraffin-embedded, cut into 5 μm-thick sections and then stained by using a periodic acid–schiff (PAS) kit (Beyotime Biotechnology, China) (Jeong & Kim, 2022). Microstructures of midgut tissues were observed by using a light microscope with 200× magnification. Goblet cell numbers and length-to-width ratios in villi were determined. The experiment was repeated in triplicate.

2.4 | Bacterial load determination and gene expressions by qRT-PCR assay

Total RNA was isolated from midgut and liver by using HiPure Total RNA Mini Kit (Magen Biotechnology, China). After RNA quality assessment, 1000 ng of purified total RNA was used for cDNA synthesis by using MonScript™ RT III All-in-One Mix with dsNase (Monad, China). Relative expressions of zonula occludens-1 (ZO-1), occludin, claudin-10, claudin-12, claudin-20, mucin 7 (MUC7), mucin 13 (MUC13), polycomb ring finger oncogene (BMI-1), CD22, CD28, metalloprotein 9 (MMP9), metalloprotein 23 (MMP23), complement component 1q (C1q), complement component 6 (C6), liver expressed antimicrobial peptide-2 (LEAP-2), Toll-like receptor 5 (TLR5), lysozyme C (LysC), caspase-2 and caspase-9 were investigated by qRT-PCR assay. 18S rRNA was used as internal control. The primer sequences are shown in Table 1.

For bacterial load determination, the above-isolated tissues were homogenized for genomic DNA extraction by using a DNA extraction kit (Magen Biotechnology, China) (Luo et al., 2020). Before detection, DNA concentration was adjusted to 100 ng/μL. Relative expression of *A. hydrophila* hlyA gene was detected by qRT-PCR assay, while GAPDH was used as reference gene. Briefly, qRT-PCR assay was performed by using PowerUp SYBR Green Master Mix (Applied Biosystems, USA) and measured by using Applied Biosystems QuantStudio 5 Real-Time PCR System with $2^{-\Delta\Delta Ct}$ methods. PCR procedure was shown below: 1 cycle of 95°C for 1 min, 40 cycles of 95°C for 30 s, 60°C for 1 min, followed by melting curve analysis for qRT-PCR confirmation. The experiments were performed in triplicate.

2.5 | Detection of antioxidant enzymes in liver

2.5.1 | Catalase (CAT) activity

Catalase activities in liver were detected at OD_{405} absorbance by using a CAT activity kit (Nanjing Jiancheng Bioengineering Institute, China). Results were given in units of CAT activity per milligram of protein, where 1 U of CAT is defined as the amount of enzyme decomposing 1 μmol H_2O_2 per second. The experiment was repeated in triplicate.

2.5.2 | Glutathione peroxidase (GPx) activity

Glutathione peroxidase activities in liver were observed at OD_{340} absorbance by using a GPx activity kit (Beyotime Biotechnology, China). Results were shown as mU GPx activity per milligram of protein. The experiment was repeated in triplicate.

2.5.3 | Glutathione reductase (GR) activity

Glutathione reductase activities in liver were detected at OD_{412} absorbance by using a GR activity kit (Beyotime Biotechnology, China). Results were presented as mU GR activity per milligram of protein. The experiment was repeated in triplicate.

TABLE 1 The primer sequences used in this study.

Primer names	Sequence direction (5′ → 3′)	Use
qpcr-zo-1-F	TGCCCAGAGGTGAA GAGGTC	qPCR
qpcr-zo-1-R	GCCCAGTTTGCCGTTGTAA	qPCR
qpcr-occludin-F	GTTGCCCATCCGTAGTT CAGT	qPCR
qpcr-occludin-R	CTTCAGCCAGACGCTTGTTG	qPCR
qpcr-claudin10-F	ATGTAGGAGGCAAG GGTGGT	qPCR
qpcr-claudin10-R	GCAGTTAGTGACGGACG AGGT	qPCR
qpcr-claudin12-cara-F	CTTGCTGCTCCAAAACT CCTG	qPCR
qpcr-claudin12-cara-R	GCCACATACACCCCAAA CTCT	qPCR
qpcr-claudin20-cara-F	GCCTAACTGGAAGG TGAGCG	qPCR
qpcr-claudin20-cara-R	GCCGTCTGGAGGTATGCG	qPCR
qpcr-MUC7-F	AGACCAAAGCCCACGCAG	qPCR
qpcr-MUC7-R	ACACCAGTCCAGCCAGCAG	qPCR
qpcr-MUC13-F	TGCCACATCAGTTTCAG TTGC	qPCR
qpcr-MUC13-R	TTCACCCACCGCCATTTC	qPCR
qpcr-BMI-1-F	TGAGGACAGAGGAGAAG TGGC	qPCR
qpcr-BMI-1-R	GCAGGGCATTGTAAGTAGCG	qPCR
qpcr-CD28-F	CAGAAAGATTGGAAACG GCACT	qPCR
qpcr-CD28-R	AGGAAGCGACGATTAGG ATGG	qPCR
qpcr-CD22-F	ACTGGATGTATGGACAA TGGC	qPCR
qpcr-CD22-R	TTGCGTAGACTGCTGAA CCTT	qPCR
qpcr-MMP23-F	AAGACGCCCGCTCCCA	qPCR
qpcr-MMP23-R	GCCAGTTCTCCAGTGATGCC	qPCR
qpcr-18S-F	CGGAGGTTCGAAGA CGATCA	qPCR
qpcr-18S-R	GAGGTTTCCCGTGTTGAGTC	qPCR
qpcr-GAPDH-F	CAGGGTGGTGCCAAGCG	qPCR
qpcr-GAPDH-R	GGGGAGCCAAGCAG TTAGTG	qPCR
qpcr-hlyA-F	GGCCGGTGGCCCGAAGA TACGGG	qPCR
qpcr-hlyA-R	GGCGGCGCCGGACGAGA CGGGG	qPCR
qpcr-casp2-F	GGCTAAACCGACATCCCAGG	qPCR
qpcr-casp2-R	GCCGTAAGAGCAGCACA GAAG	qPCR
qpcr-casp9-F	GTGGGATAGATGACCAG ACGG	qPCR
qpcr-casp9-R	GAGAAGTTTTCGGAGGA AGTTGA	qPCR
qPCR-MMP9-F	GACATCCGCAACTATCA AACTT	qPCR
qPCR-MMP9-R	GGGGTAACATCACTCCA GACTT	qPCR
qpcr-TLR5-F	GAAACCTTCAACCTGGCTCA	qPCR
qpcr-TLR5-R	ATCCTGGCTGTCGTCGG	qPCR
qpcr-C1q-F	GTGGTGGCATTGATGGCAG	qPCR
qpcr-C1q-R	TCGGTTTCGCAGCACAGAG	qPCR
qpcr-C6-F	GAGCCAAGCATCCCACAAG	qPCR
qpcr-C6-R	TGAGCAGGTCTCCCATTCG	qPCR
qpcr-leap2-F1	AGACACTGACTGGGCGACC	qPCR
qpcr-leap2-R1	CTGTTGAGCATTATTGA AGGA	qPCR
qpcr-lysC-F	ATGAAGGTGGCGATTGCG	qPCR
qpcr-lysC-R	AAACTTGCTTTCCCAGT AGGC	qPCR

(Continues)

TABLE 1 (Continued)

2.6 | Statistical analyses

The above results were subjected to one-way ANOVA analysis by using SPSS. If the analytical levels of *p*-value reach <.05, results were statistically significant.

3 | RESULTS

3.1 | Pathological characteristics of midgut villi after *A. hydrophila* challenge

In Figure 1a–g, a significant morphological alteration was detected in midgut of WCC following gut infection with *A. hydrophila*. Villi vacuolization was observed in midgut at 24 h post-infection, then midgut villi showed a deformed characteristics with abnormal cell morphology, fusion and submucosal rupture, whereas no pathological change was observed in the control. In Figure 1h, the average numbers of Goblet cells in *A. hydrophila*-infected midgut were consistently higher than those of the control, while time-dependent reduction of length-to-width ratios of midgut villi was observed (Figure 1i).

3.2 | Bacterial load detection

In Figure 2a–d, expression profiles of *A. hydrophila* hlyA gene in liver, kidney and midgut peaked at 24 h post-infection, followed by a significant decline from 24 h to 72 h, while highest level of *A. hydrophila* hlyA gene expression in spleen was detected at 48 h post-infection.

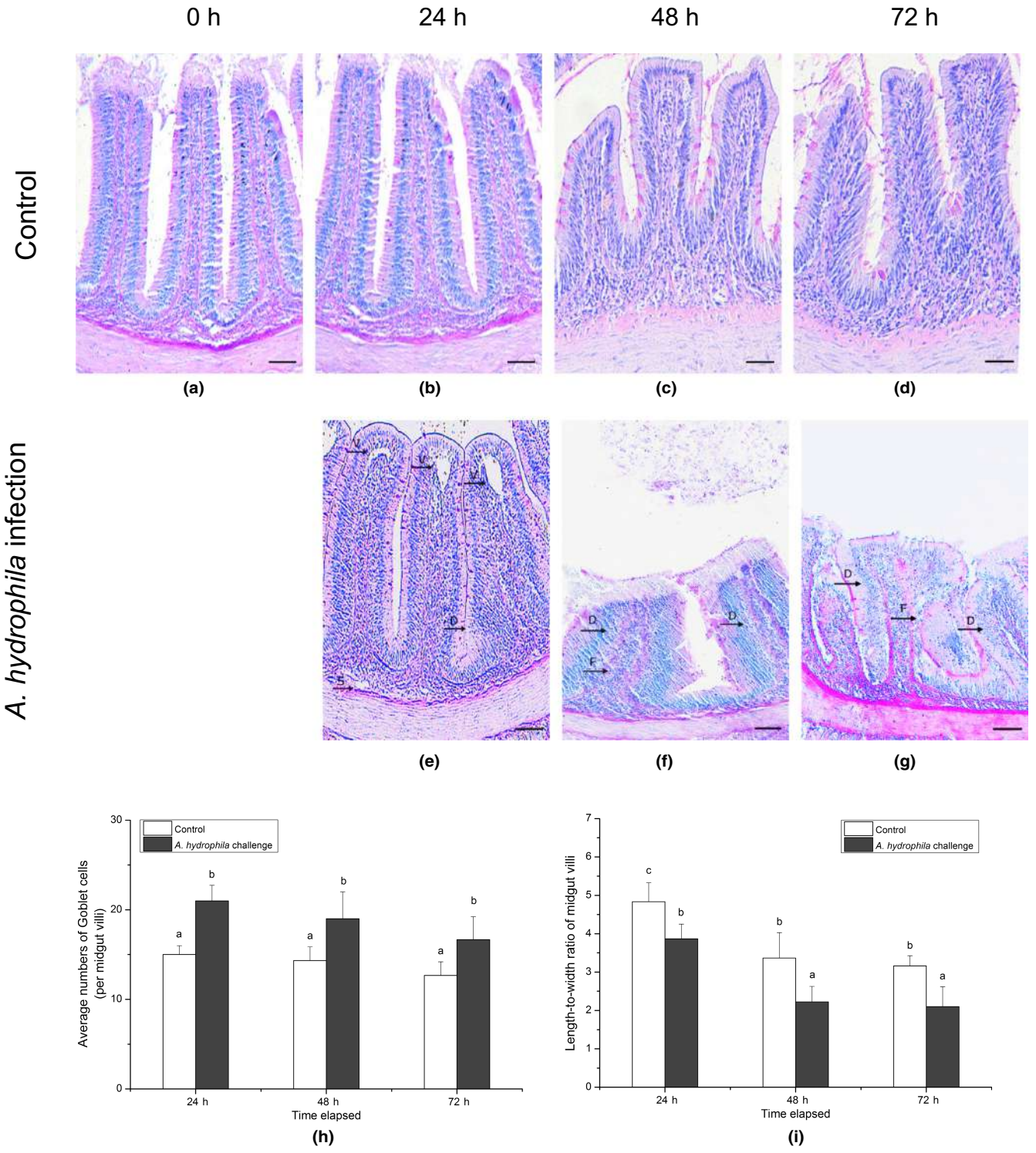

FIGURE 1 Morphological analysis of midgut in WCC anally intubated with *A. hydrophila*. (a–g) Histological section of midgut treated with *A. hydrophila* at 24 h, 48 h and 72 h, while PBS treatment was used as control group. E: edema of midgut wall; H: goblet cell hyperplasia; D: villi deformation; V: villus vacuolization; S: submucosal rupture; F: villus fusion. (h, i) average numbers of goblet cells and length-to-width ratio of midgut villi were calculated. Results (mean ± SD) with different letters were significantly different ($p < .05$). The experiments were performed in triplicate.

3.3 | Expressions of tight junction proteins and immune-related genes in midgut

As shown in Figure 3a–e, WCC anally intubated with *A. hydrophila* exhibited a significant decline of ZO-1, occludin, claudin-10, claudin-12 and claudin-20 expression in midgut from 24 h to 72 h by comparing with the control, respectively.

In Figure 4a, MUC7 expression began to increase at 24 h post-infection and peaked at 48 h with the highest value of 19.88-fold greater than that of the control. In Figure 4b–e, expression levels

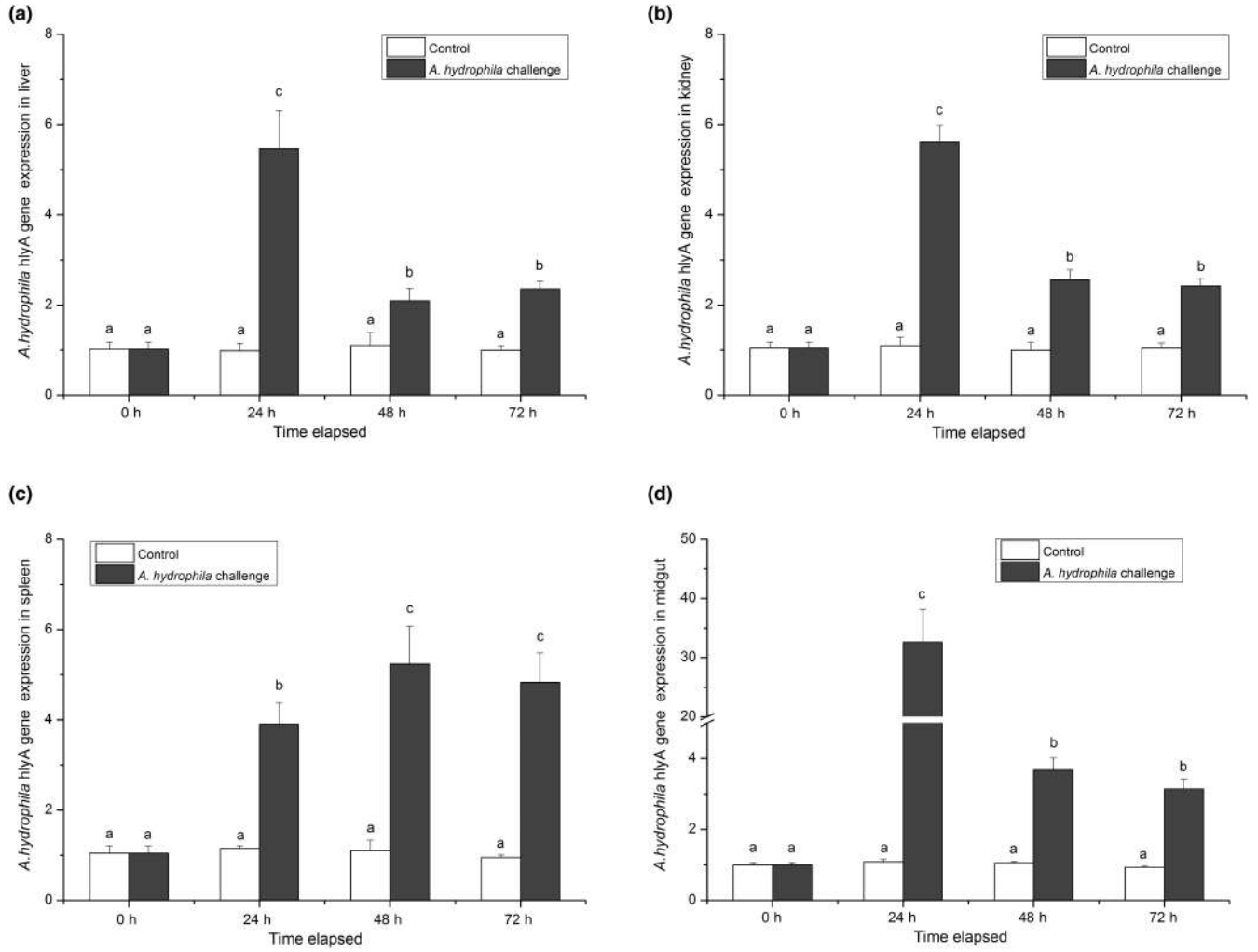

FIGURE 2 Detection of *A. hydrophila* hlyA gene expression in liver (a), kidney (b), spleen (c) and midgut (d) at 24 h, 48 h and 72 h following gut infection with *A. hydrophila*. The calculated data (mean ± SD) with different letters were significantly different ($p < .05$).

of MUC13, CD22 and CD28 reached the highest levels at 24 h post-infection, while the highest level of BMI-1 expression was observed at 72 h following gut infection with *A. hydrophila*.

3.4 | Effect of invasive *A. hydrophila* on immune and antioxidant properties in liver

As shown in Figure 5a,b, a gradual increase of liver C1q mRNA expression was observed from 24 h to 72 h following gut infection with *A. hydrophila*, whereas liver C6 expression peaked at 48 h, followed by a dramatic decline. In Figure 5c,d, a 48.61- and 5.82-fold increase in MMP9 and MMP23 expression was detected at 24 h and 48 h, respectively. In Figure 5e,f, caspase-2 mRNA expression increased sharply at 48 h post-infection, followed by a significant decline at 72 h, while caspase-9 expression reached the highest level at 24 h and declined gradually from 24 h to 72 h. In Figure 5g–i, the highest expression profiles of TLR5, LEAP-2 and LysC in *A. hydrophila*-infected WCC were approximately 45.32-, 4.36- and 12.18-fold greater than those of the control, respectively. In Figure 5j–l, enzymatic activities of CAT, GPx and GR in liver reached the peaked levels at 72 h post-infection, respectively.

4 | DISCUSSION

Aeromonas hydrophila is widely considered as one of major etiologic agents in aqueous environments, which can trigger a wide spectrum of diseases such as gastroenteritis and septicemia (Abd-El-Malek, 2017). Most isolated *A. hydrophila* strains can exert the cytotoxic effect and possess a quantity of virulence factors, including enterotoxin, haemolysin and cytotoxin (Gray et al., 1990). Furthermore, alternative sigma factors, two-component systems, heat shock proteins and cold shock proteins of *A. hydrophila* can directly participate in stress response mechanisms, which can enable biofilm formation and maturation to enhance its ability of food- and water-borne pathogens and survive in environment or within the host (Awan et al., 2018).

Our previous findings have demonstrated that invasive *A. hydrophila* can alleviate antioxidant status and impair metabolic

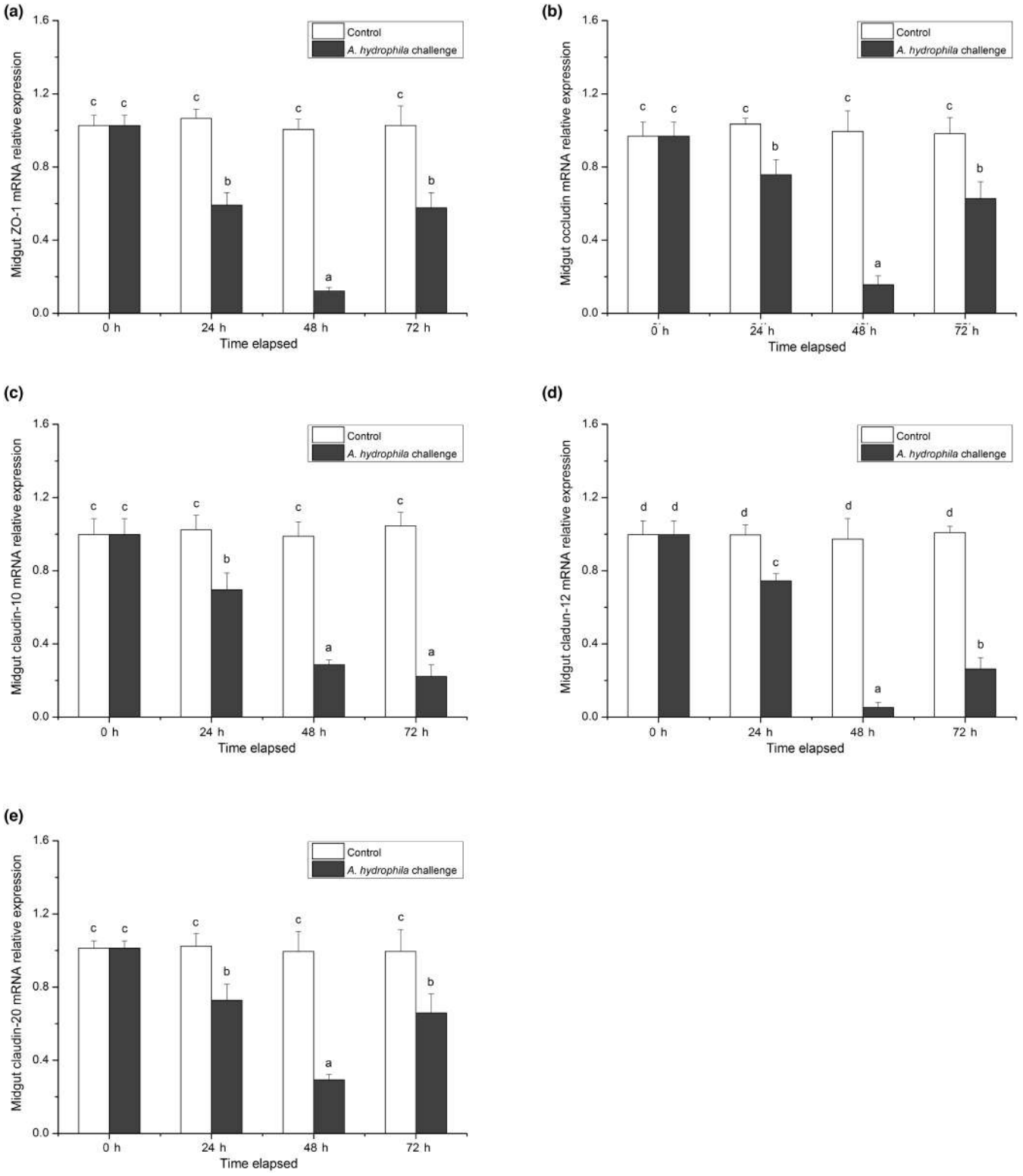

FIGURE 3 Effect of *A. hydrophila* infection on tight junction. Expression profiles of ZO-1 (a), occludin (b), claudin-10 (c), claudin-12 (d) and claudin-20 (e) were determined in midgut of WCC following *A. hydrophila* infection. The calculated data (mean ± SD) with different letters were significantly different ($p < .05$) among the groups. The experiments were performed in triplicate.

homeostasis in fish kidney (Xiong et al., 2023). In this current study, WCC receiving anal intubation with *A. hydrophila* showed a progressive pathological characteristics with severe tissue deformation and abnormal cell morphology in midgut villi, along with an increased numbers of goblet cells. In general, tight junction integrity acting as physiological barrier is playing an important role in the frontline defence against infectious agents (Schneeberger & Lynch, 2004), while epithelial cells is pivotal sensors of invading microbes in gut

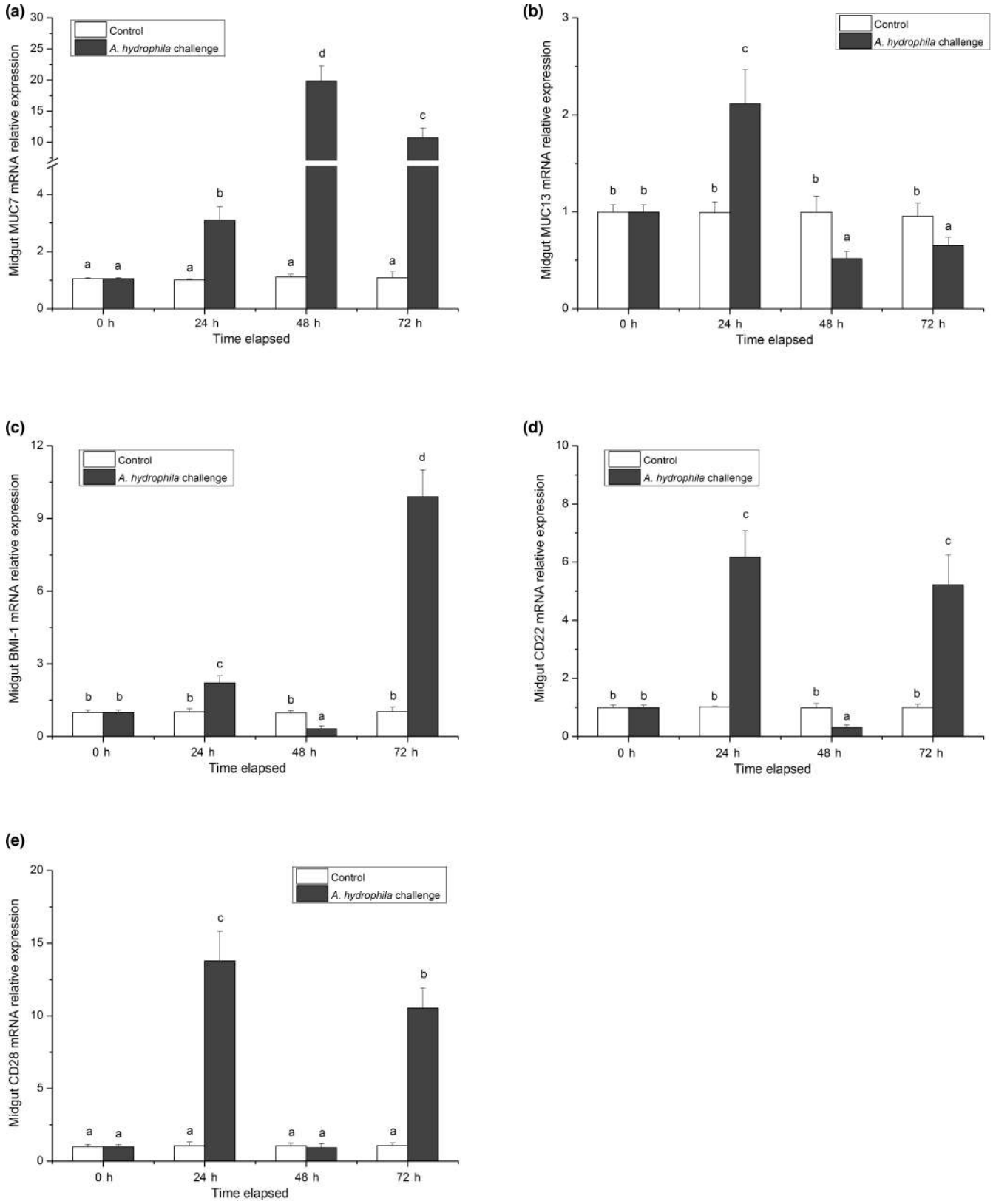

FIGURE 4 Gene expressions in midgut mucosal immunity of WCC anally intubated with *A. hydrophila*. Expressions of MUC7 (a), MUC13 (b), BMI-1 (c), CD22 (d) and CD28 (e) were detected by qRT-PCR assay. The calculated data (mean ± SD) with different letters were significantly different ($p < .05$) among the groups. The experiments were performed in triplicate.

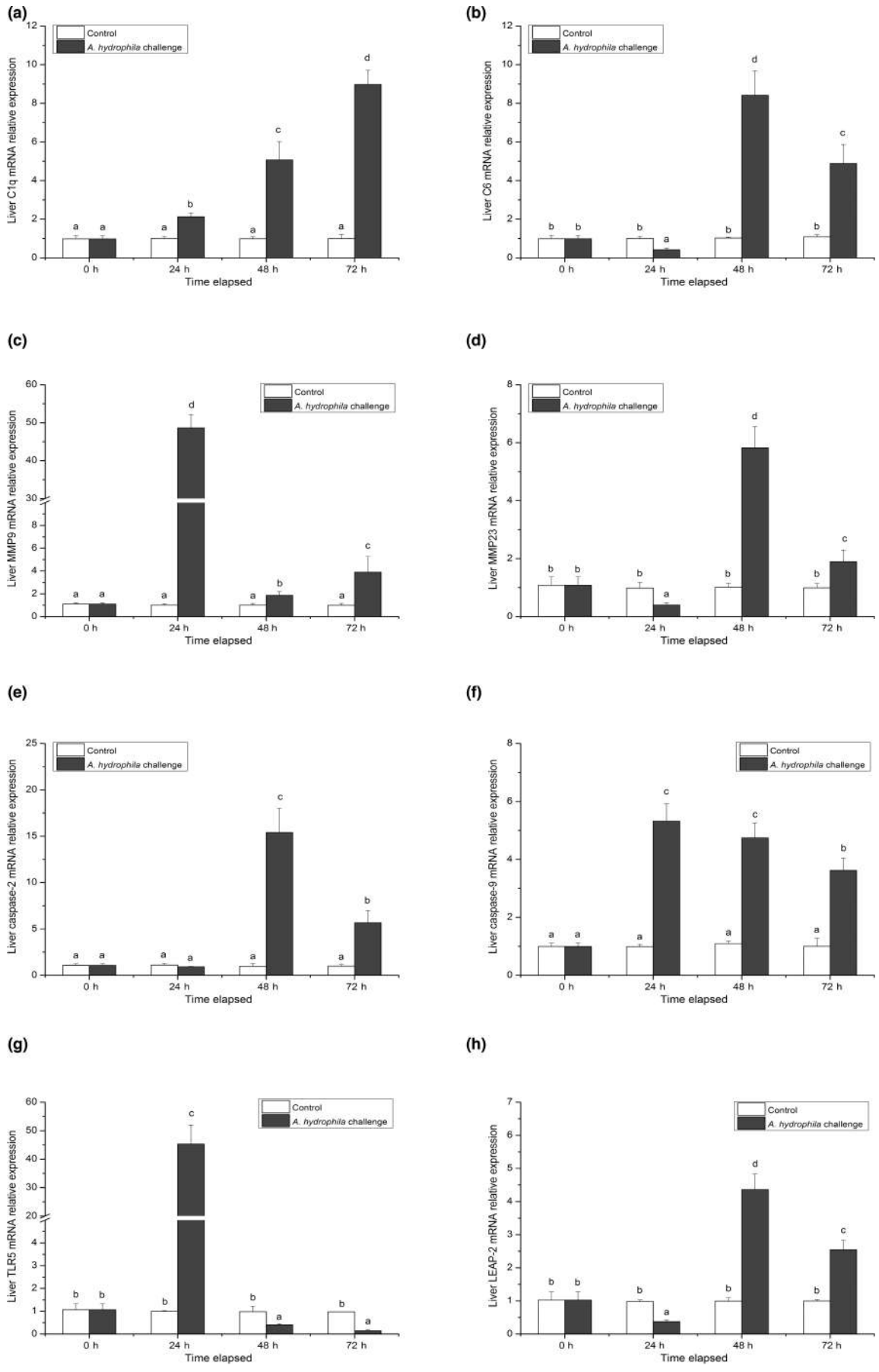

FIGURE 5 (Continued)

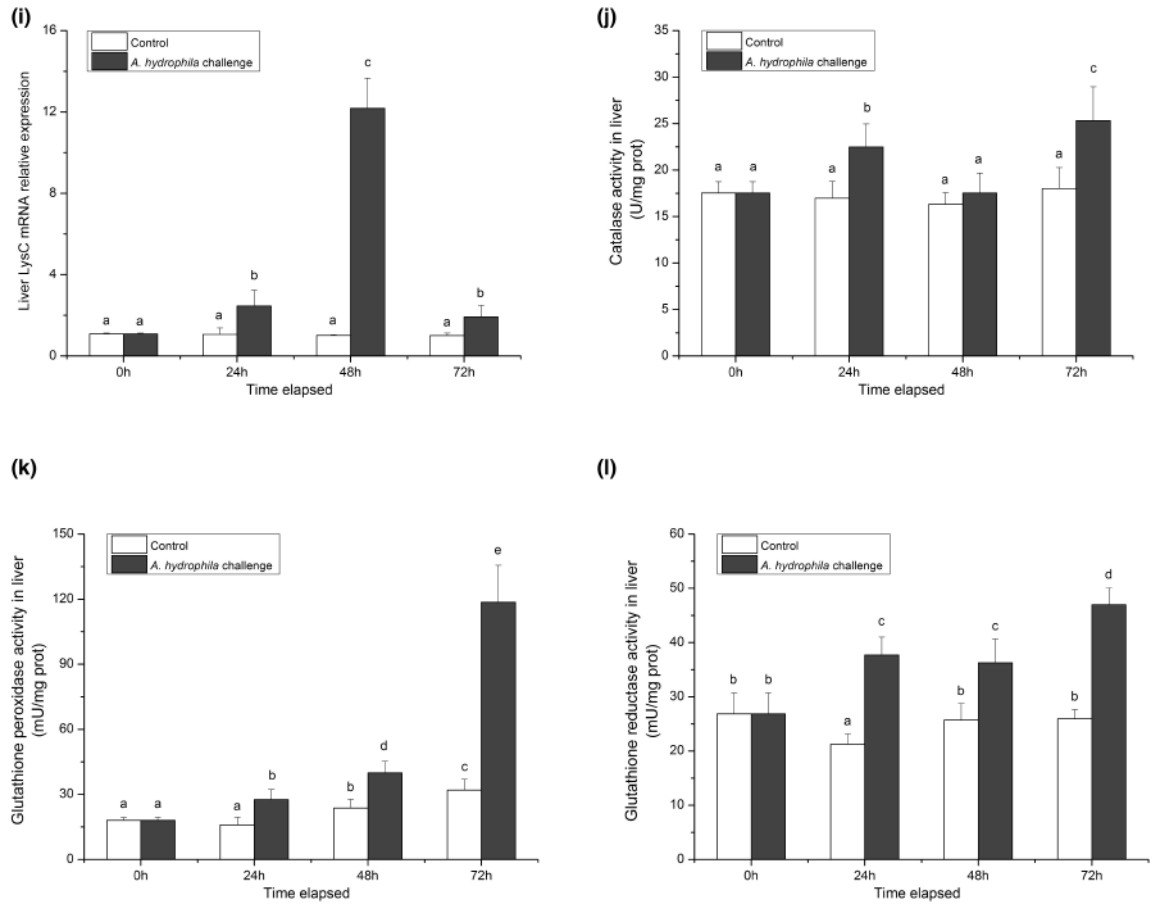

FIGURE 5 Assessment of immune-related gene expressions and antioxidant properties in liver of WCC anally intubated with *A. hydrophila*. (a–i) Expressions of C1q, C6, MMP9, MMP23, caspase-2, caspase-9, TLR-5, LEAP-2 and LysC were detected by qRT-PCR assay. (j–l) Enzymatic activities of CAT, GPx and GR were determined in liver. The calculated data (mean ± SD) with different letters were significantly different ($p < .05$) among the groups. The experiments were performed in triplicate.

tract, which can recruit and chemoattract the adhesion of activated immune cells (Kagnoff & Eckmann, 1997). Mucus layer and goblet cells can direct mucosal immune defence against invasive pathogens and facilitate immune-related cell connection in gut tract by secreting mucin glycoproteins and bioactive molecules (Kim & Ho, 2010; Pelaseyed et al., 2014). BMI-1 belonging to polycomb-repressive complex 1 (PRC1) family is indispensable for self-renewal and maintenance of stem cells in gut tract, which may facilitate overall tissue homeostasis and repair (Bhattacharya et al., 2015). CD22 is a transmembrane glycoprotein that regulates a central role in the survival and cellular homeostasis of mature B lymphocytes (Tedder et al., 2005). CD28, a member of heterophilic cell adhesion complex, can bind to B7 molecule on antigen-presenting cells, then modulating T lymphocyte activation and cytokine production (June et al., 1990). In this study, WCC anally intubated with *A. hydrophila* showed a declined level of ZO-1, occludin, claudin-10, claudin-12 and claudin-20 in midgut, along with elevated profiles of MUC7, MUC13, BMI-1, CD22 and CD28. Additionally, expressions of *A. hydrophila* hlyA increased significantly in liver, kidney, spleen and midgut of WCC subjected to gut infection with *A. hydrophila*. These results implied that *A. hydrophila* infection promote midgut injury with increased levels of mucosal immune response and epithelial permeability, leading to the migration of invasive *A. hydrophila to* other tissues for systemic infection through gut barrier.

Liver is one of major recipients of gut-derived products, which enables production of acute phase proteins and antimicrobial molecules to alleviate the dispersal of infectious agents, mitigate tissue injury and participate in immune surveillance (Bayne & Gerwick, 2001). Moreover, liver is also playing a predominant role in eliminating invasive pathogens by generating 80% to 90% of the complement components and pattern-recognition receptors (Gao et al., 2008). C1q is a critical complement component that can exert in vitro antibacterial activity and modulate the activation of classical complement cascades (Wang et al., 2017). C6 is one of important terminal complement components involved in formation of membrane attack complex (MAC), which can enable formation of C5b-9 complex to promote complement-mediated lysis (Schäfer et al., 1986). MMPs are zinc-dependent endopeptidases that can confer protection against lethal bacterial infection in fish by regulating macrophage migration (Shan et al., 2016). LEAP-2 and LysC are involved in direct bacteria killing mechanism in fish (Li et al., 2015; Wei et al., 2012). CAT, GR and GPx are playing

an important role in first line of antioxidant defence against free radicals during pathogenic infection (Sahreen et al., 2021), but prolonged production of reactive oxygen species (ROS), one of potent antibacterial molecules, can induce antioxidant insult, impair macromolecular bioactivity as well as promote cell death via caspase signals (Ricci et al., 2003; Rizwan et al., 2014). In this study, elevated expressions of C1q, C6, MMP9, MMP23, TLR5, LEAP-2, LysC, caspase-2 and caspase-9 were detected in liver of WCC anally intubated with *A. hydrophila*, along with up-regulation of CAT, GR and GPx activity. Thus, taken together, these results indicated that midgut infection with *A. hydrophila* could trigger systemic immune response and antioxidant alternation in gut–liver axis of WCC.

In summary, we characterized time-dependent midgut damage and increased levels of bacterial loads in tissues of WCC subjected to gut infection with *A. hydrophila*. Gut infection with *A. hydrophila* could increase midgut epithelial permeability and reduce expression levels of tight junction proteins, but immune signals in gut mucosal barrier were activated. In addition, elevated levels of immune-related gene expressions and antioxidant capacities were detected in liver. Thus, the information presented in this study could give a new insight into the immune regulation in gut–liver axis of WCC undergoing gut infection with *A. hydrophila*.

AUTHOR CONTRIBUTIONS

Fei Wang performed methodology and formal analysis. Zi-Le Qin and Wei-Sheng Luo performed methodology. Ning-Xia Xiong and Jie Ou performed formal analysis and verification. Ming-Zhu Huang performed Conceptualization. Sheng-Wei Luo performed Conceptualization, supervision, project management and article writing. Shao-Jun Liu performed supervision. The authors of this manuscript are all aware of the journal to which the manuscript was submitted, and all agree to continue to support the follow-up work.

FUNDING INFORMATION

This research was supported by the National Natural Science Foundation of China, China (grant no. 31902363), Hunan Provincial Natural Science Foundation of China, China (grant no. 2021JJ40340).

CONFLICT OF INTEREST STATEMENT

The authors declare that they have no conflict of interest.

DATA AVAILABILITY STATEMENT

The authors confirm that the data supporting the findings of this study are available within the article [and/or] its supplementary materials.

REFERENCES

Abd-El-Malek, A. M. (2017). Incidence and virulence characteristics of Aeromonas spp. in fish. *Veterinary World*, *10*, 34–37.

Awan, F., Dong, Y., Wang, N., Liu, J., Ma, K., & Liu, Y. (2018). The fight for invincibility: Environmental stress response mechanisms and Aeromonas hydrophila. *Microbial Pathogenesis*, *116*, 135–145.

Bayne, C. J., & Gerwick, L. (2001). The acute phase response and innate immunity of fish. *Developmental & Comparative Immunology*, *25*, 725–743.

Bhattacharya, R., Mustafi, S. B., Street, M., Dey, A., & Dwivedi, S. K. D. (2015). Bmi-1: At the crossroads of physiological and pathological biology. *Genes & Diseases*, *2*, 225–239.

Dong, H., Chen, Y., Wang, J., Zhang, Y., Zhang, P., Li, X., Zou, J., & Zhou, A. (2020). Interactions of microplastics and antibiotic resistance genes and their effects on the aquaculture environments. *Journal of Hazardous Materials*, *403*, 123961.

Ellis, A. (1999). Immunity to bacteria in fish. *Fish & Shellfish Immunology*, *9*, 291–308.

Gao, B., Jeong, W. I., & Tian, Z. (2008). Liver: An organ with predominant innate immunity. *Hepatology*, *47*, 729–736.

Gray, S., Stickler, D., & Bryant, T. (1990). The incidence of virulence factors in mesophilic Aeromonas species isolated from farm animals and their environment. *Epidemiology & Infection*, *105*, 277–294.

Jeong, M. K., & Kim, B.-H. (2022). Grading criteria of histopathological evaluation in BCOP assay by various staining methods. *Toxicological Research*, *38*, 9–17.

June, C. H., Ledbetter, J. A., Linsley, P. S., & Thompson, C. B. (1990). Role of the CD28 receptor in T-cell activation. *Immunology Today*, *11*, 211–216.

Kagnoff, M. F., & Eckmann, L. (1997). Epithelial cells as sensors for microbial infection. *The Journal of Clinical Investigation*, *100*, 6–10.

Kelly, D., Conway, S., & Aminov, R. (2005). Commensal gut bacteria: Mechanisms of immune modulation. *Trends in Immunology*, *26*, 326–333.

Kim, Y. S., & Ho, S. B. (2010). Intestinal goblet cells and mucins in health and disease: Recent insights and progress. *Current Gastroenterology Reports*, *12*, 319–330.

Li, B., Selmi, C., Tang, R., Gershwin, M., & Ma, X. (2018). The microbiome and autoimmunity: A paradigm from the gut–liver axis. *Cellular & Molecular Immunology*, *15*, 595–609.

Li, H.-X., Lu, X.-J., Li, C.-H., & Chen, J. (2015). Molecular characterization of the liver-expressed antimicrobial peptide 2 (LEAP-2) in a teleost fish, *Plecoglossus altivelis*: Antimicrobial activity and molecular mechanism. *Molecular Immunology*, *65*, 406–415.

Li, Z., Wang, Z. W., Wang, Y., & Gui, J. F. (2018). Crucian carp and gibel carp culture. *Aquaculture in China: Success Stories and Modern Trends*, 149–157.

Luo, S.-W., Luo, Z.-Y., Yan, T., Luo, K.-K., Feng, P.-H., & Liu, S.-J. (2020). Antibacterial and immunoregulatory activity of a novel hepcidin homologue in diploid hybrid fish (*Carassius auratus cuvieri*♀ × *Carassius auratus* red var♂). *Fish & Shellfish Immunology*, *98*, 551–563.

Nielsen, M. E., Høi, L., Schmidt, A., Qian, D., Shimada, T., Shen, J., & Larsen, J. (2001). Is Aeromonas hydrophila the dominant motile Aeromonas species that causes disease outbreaks in aquaculture production in the Zhejiang Province of China? *Diseases of Aquatic Organisms*, *46*, 23–29.

Pelaseyed, T., Bergström, J. H., Gustafsson, J. K., Ermund, A., Birchenough, G. M., Schütte, A., van der Post, S., Svensson, F., Rodríguez-Piñeiro, A. M., & Nyström, E. E. (2014). The mucus and mucins of the goblet cells and enterocytes provide the first defense line of the gastrointestinal tract and interact with the immune system. *Immunological Reviews*, *260*, 8–20.

Ricci, J.-E., Gottlieb, R. A., & Green, D. R. (2003). Caspase-mediated loss of mitochondrial function and generation of reactive oxygen species during apoptosis. *The Journal of Cell Biology*, *160*, 65–75.

Rizwan, S., ReddySekhar, P., & MalikAsrar, B. (2014). Reactive oxygen species in inflammation and tissue injury. *Antioxidants & Redox Signaling*, *20*(7), 1126–1167.

Rodger, H. D. (2016). *Fish disease causing economic impact in global aquaculture, fish vaccines* (pp. 1–34). Springer.

Sahreen, A., Fatima, K., Zainab, T., & Saifullah, M. K. (2021). Changes in the level of oxidative stress markers in Indian catfish (*Wallago attu*) infected with *Isoparorchis hypselobagri*. *Beni-Suef University Journal of Basic and Applied Sciences*, *10*, 1–8.

Schäfer, H., Mathey, D., Hugo, F., & Bhakdi, S. (1986). Deposition of the terminal C5b-9 complement complex in infarcted areas of human myocardium. *The Journal of Immunology*, *137*, 1945–1949.

Schneeberger, E. E., & Lynch, R. D. (2004). The tight junction: A multifunctional complex. *American Journal of Physiology-Cell Physiology*, *286*, C1213–C1228.

Secombes, C., Wang, T., Hong, S., Peddie, S., Crampe, M., Laing, K., Cunningham, C., & Zou, J. (2001). Cytokines and innate immunity of fish. *Developmental & Comparative Immunology*, *25*, 713–723.

Seo, Y. S., & Shah, V. H. (2012). The role of gut-liver axis in the pathogenesis of liver cirrhosis and portal hypertension. *Clinical and Molecular Hepatology*, *18*, 337–346.

Shan, Y., Zhang, Y., Zhuo, X., Li, X., Peng, J., & Fang, W. (2016). Matrix metalloproteinase-9 plays a role in protecting zebrafish from lethal infection with listeria monocytogenes by enhancing macrophage migration. *Fish & Shellfish Immunology*, *54*, 179–187.

Song, X., Zhao, J., Bo, Y., Liu, Z., Wu, K., & Gong, C. (2014). Aeromonas hydrophila induces intestinal inflammation in grass carp (*Ctenopharyngodon idella*): An experimental model. *Aquaculture*, *434*, 171–178.

Tedder, T. F., Poe, J. C., & Haas, K. M. (2005). CD22: A multifunctional receptor that regulates B lymphocyte survival and signal transduction. *Advances in Immunology*, *88*, 1–50.

Uribe, C., Folch, H., Enríquez, R., & Moran, G. (2011). Innate and adaptive immunity in teleost fish: A review. *Veterinární Medicína*, *56*, 486–503.

Wang, L., Fan, C., Xu, W., Zhang, Y., Dong, Z., Xiang, J., & Chen, S. (2017). Characterization and functional analysis of a novel C1q-domain-containing protein in Japanese flounder (*Paralichthys olivaceus*). *Developmental & Comparative Immunology*, *67*, 322–332.

Warner, K., Hamza, M., Oliver-Smith, A., Renaud, F., & Julca, A. (2010). Climate change, environmental degradation and migration. *Natural Hazards*, *55*, 689–715.

Wei, S., Huang, Y., Cai, J., Huang, X., Fu, J., & Qin, Q. (2012). Molecular cloning and characterization of c-type lysozyme gene in orange-spotted grouper, *Epinephelus coioides*. *Fish & Shellfish Immunology*, *33*, 186–196.

Wen, L., Yang, C., Liao, X., Zhang, Y., Chai, X., Gao, W., Guo, S., Bi, Y., Tsang, S.-Y., & Chen, Z.-F. (2022). Investigation of PM2. 5 pollution during COVID-19 pandemic in Guangzhou, China. *Journal of Environmental Sciences*, *115*, 443–452.

Xiong, N.-X., Fang, Z.-X., Kuang, X.-Y., Ou, J., Luo, S.-W., & Liu, S.-J. (2023). Integrated analysis of gene expressions and metabolite features unravel immunometabolic interplay in hybrid fish (*Carassius cuvieri*♀× *Carassius auratus* red var♂) infected with *Aeromonas hydrophila*. *Aquaculture*, *563*, 738981.

Xiong, N.-X., Ou, J., Fan, L.-F., Kuang, X.-Y., Fang, Z.-X., Luo, S.-W., Mao, Z.-W., Liu, S.-J., Wang, S., & Wen, M. (2022). Blood cell characterization and transcriptome analysis reveal distinct immune response and host resistance of different ploidy cyprinid fish following Aeromonas hydrophila infection. *Fish & Shellfish Immunology*, *120*, 547–559.

How to cite this article: Wang, F., Qin, Z.-L., Luo, W.-S., Xiong, N.-X., Huang, M.-Z., Ou, J., Luo, S.-W., & Liu, S.-J. (2023). Alteration of synergistic immune response in gut–liver axis of white crucian carp (*Carassius cuvieri*) after gut infection with *Aeromonas hydrophila*. *Journal of Fish Diseases*, *00*, 1–11. https://doi.org/10.1111/jfd.13799